[5] Cf. A. KLEMM, Z. Naturforsch. **1**, 252 [1946].
[6] A. LUNDÉN and A. EKHED, Z. Naturforsch. **24 a**, 892 [1969].
[7] A. LUNDÉN and A. EKHED, Z. Naturforsch. **23 a**, 1779 [1968].
[8] I. OKADA, Thesis, Tokyo University 1966.
[9] A. LUNDÉN, Z. Naturforsch. **21 a**, 1510 [1966].
[10] A. LUNDÉN, Z. Naturforsch. **14 a**, 801 [1959].
[11] F. R. DUKE and B. OWENS, J. Electrochem. Soc. **105**, 548 [1958].
[12] E. P. HONIG and J. A. A. KETELAAR, Trans. Faraday Soc. **62**, 190 [1966].
[13] S. C. WAIT and A. T. WARD, J. Chem. Phys. **44**, 448 [1966]; S. C. WAIT, A. T. WARD, and G. J. JANZ, J. Chem. **45**, 133 [1966].
[14] K. WILLIAMSON, P. LI, and J. P. DEVLIN, J. Chem. Phys. **48**, 3891 [1968].
[15] G. H. WEGDAM, R. BONN, and J. VAN DER ELSKEN, Chem. Phys. Letters **2**, 182 [1968].
[16] Equation (9) is derived either from Equation (8) or easily from the equation presented by A. KLEMM, Z. Naturforsch. **3 a**, 127 [1948].
[17] S. JORDAN and A. KLEMM, Z. Naturforsch. **21 a**, 1584 [1966].
[18] The activation energy is evaluated from the data of B. DE NOOIJER, Thesis, University of Amsterdam 1965.
[19] A. S. DWORKIN, R. B. ESCUE, and E. R. VAN ARTSDALEN, J. Phys. Chem. **64**, 872 [1960].
[20] A. LUNDÉN, A. FLOBERG, and R. MATSSON, to be published.
[21] For $LiNO_3$, the temperature dependence of μ_{int} has been measured in two laboratories, see Refs. [6] and [8], the result being that the mass effect either is independent of the temperature [6], or that it decreases slightly when the temperature increases [8]. Possible causes of the discrepancy are discussed in Ref. [6].

Dissociation Lifetimes of Molecular Ions Produced by Charge Exchange *

B. ANDLAUER ** and CH. OTTINGER ***

Physikalisches Institut der Universität Freiburg, Germany

(Z. Naturforsch. **27 a**, 293—309 [1972]; received 27 November 1971)

Ions of the benzonitrile, benzene and thiophene molecules were produced in well-defined states of excitation by charge exchange with Xe^+, Kr^+, Ar^+, CO^+, and N_2^+. Their subsequent unimolecular decomposition was followed, as a function of time, by allowing the dissociations to take place within a strong homogeneous draw-out field and measuring the kinetic energy of the product ions. The decompositions were found to be purely exponential within experimental error, and the corresponding decay rate constants k (for $2 \cdot 10^5$ sec$^{-1} \leqq k \leqq 5 \cdot 10^8$ sec^{-1}) proved to be monotonically increasing functions of the excitation energy. These are the first unambiguous measurements of this function $k(E)$ for any molecule. In the case of benzene, the reactions $C_6H_6^+ \rightarrow C_6H_5^+ + H$ and $C_6H_6^+ \rightarrow C_4H_4^+ + C_2H_2$ were found to be definitely not in competition with one another. Furthermore the dependence of the excitation energy on the impact energy was measured. A variation of the impact energy between 10 and 200 $eV_{c.m.}$ only changes the internal energy E by about 0.1 eV. This value appears to be in qualitative agreement with calculations on near-resonant charge transfer by Gurnee and Magee.

I. Introduction

Unimolecular decompositions of excited polyatomic ions play an important role in many radiochemical and radiobiological systems as well as in organic mass spectrometry. An understanding of the host of possible concurrent and consecutive reactions has to be founded on a consistent picture of the time scale as well as the energetics of the unimolecular processes. Today still very little is known about the decomposition rate constant k of isolated excited ions, and even less about the dependence of k on the excitation energy E. In principle the function $k(E)$ can be calculated within the framework of the quasi-equilibrium theory, henceforth abbreviated as QET [1]. However, the great number of assumptions necessary for any such calculation makes an experimental determination of $k(E)$ highly desirable. In previous communications [2, 3] we have reported on a method for measuring, in a well-defined manner, the decomposition rate of ions produced by electron impact. Subsequently we have been able, by means of varying the electron energy, to extract from these measurements $k(E)$ for a few decompositions of benzonitrile, butane and heptane ions [4, 5]. However, this

* This work is a summary of the Diplomarbeit of B. ANDLAUER, Universität Freiburg 1970.
** Present address: Institut für Angewandte Festkörperphysik, Freiburg.
*** Present address: Max-Planck-Institut für Strömungsforschung, Göttingen.

derivation of $k(E)$ was not quite unambiguous due to the fact that electron impact always produces ions possessing a wide and largely unknown spectrum of excitation energies. This disadvantage can be overcome by using charge exchange ionization. Lindholm has shown that charge exchange is capable of producing ions in monoenergetic levels of excitation [6]. Combining Lindholm's method of well-defined excitation with our technique of measuring decomposition rates should therefore give definite information on $k(E)$.

In the present work we report on experiments of this type on the benzonitrile, benzene and thiophene ions. They constitute, to our knowledge, the first direct measurements of $k(E)$ for any ions [7]. [For decomposition of neutrals, RABINOVITCH has determined $k(E)$ in a completely different way [8].] At the same time very accurate information was obtained on the amount of kinetic energy that is converted into excitation of the target in charge exchange processes. It is found to be small (though measurable), which a posteriori provides a sound basis for the "monoenergetic" excitation method. In a few cases the variation of the charge exchange cross section with initial kinetic energy was also measured.

II. Principle of Measurement

The decomposition rate constant k was measured by relating it, or rather the mean parent ion lifetime $\tau = 1/k$, to the fragment ion kinetic energy in the following way (for details see [3]). Ionization takes place within a strong homogeneous draw-out field. The gas under investigation (e. g. benzonitrile) traverses this field in a very narrow molecular beam which coincides with an equipotential surface. Thus all ions are initially formed at the potential of this particular surface. An energy selector placed behind the exit of the ion source then records a kinetic energy distribution of the ions which simply reflects the gas density profile of the beam measured perpendicular to the ionization equipotential surface, with the draw-out field strength as a scale factor. However, this is only true for the parent ions M_0^+ (of mass m_0) of the target gas. For any fragment mass m_1 the kinetic energy distribution is distorted from that profile to the low-energy side. Figure 1 illustrates schematically this change of peak shape, shift of the peak

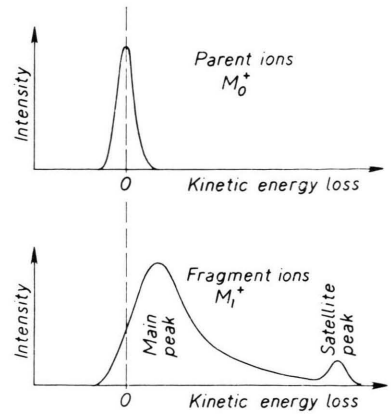

Fig. 1. Schematic kinetic energy distributions of parent and fragment ions for the unimolecular process $M_0^+ \rightarrow M_1^+ + \Delta M$, assuming formation of parent ions M_0^+ at a well-defined potential only (zero point, upper figure). M_1^+ ions appear at lower kinetic energies, the energy loss being due to ΔM split off in flight.

center and the development of a "tail". A fragment ion which is formed from a parent ion with a delay t after the initial ionization, only retains the fraction m_1/m_0 of the kinetic energy which the parent ion had at the instant of decomposition. This energy deficit increases proportionally to t^2. Thus, the low energy component of the energy distribution of mass m_1 ions is related to the distribution of lifetimes t and hence to the desired distribution $II(k)$. Of great practical importance is the draw-out field strength, F. For small F, only small values of k produce a noticeable peak distortion, while for the detection of contributions from large k high values of F are necessary. With our apparatus values of k ranging from $2 \cdot 10^5$ to $2 \cdot 10^8$ sec^{-1} can be measured.

In addition to the low energy tail on the beam profile peak, the energy distribution exhibits another, so-called satellite peak at still lower energy. It results from decompositions in the field-free region outside the ion source and is the analog on the energy scale of the classical "metastable peaks" on the mass scale. Both "main peak" distortion and relative satellite peak intensities were used in the analysis (see Sect. V).

III. Experimental

The apparatus has been described in detail in [3]. Figure 2 gives a schematic of the ion source. The essential element is a planar disc-shaped molecular beam of the target gas. It is defined by the concentric circu-

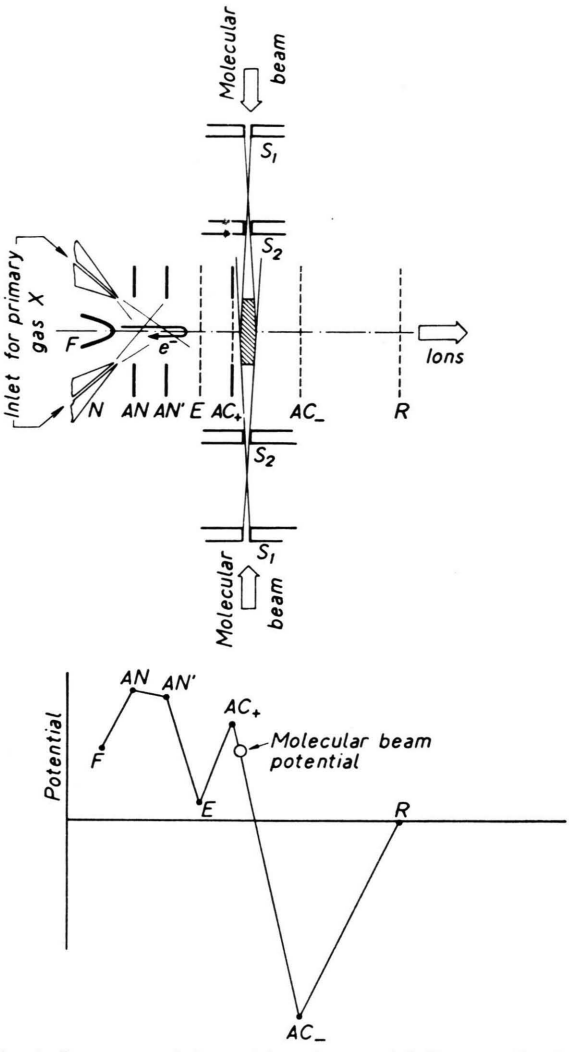

Fig. 2. Ion source (schematic) and potential diagram. S_1, S_2 = beam slits; N = primary gas inlet; F = filament; AN, AN′ = anodes; E = electron barrier electrode; AC_+, AC_-, R = ion acceleration and retardation electrodes.

lar slits S_1 and S_2. Its width on the center-line can be made as narrow as 10 μ, but for the present work $70-90\,\mu$ was used. The elements to the left of AC_+ form the auxiliary ion source to produce the primary ions and replace the electron gun used in the earlier experiments. The gas inlet into the auxiliary source is through the conical nozzle N. Electrons from the filament F ionize this gas between the anode AN and the electrode AN′ which is a few volts negative with respect to AN. The potential difference AN − AN′ is dictated by a compromise between draw-out efficiency and energy spread of the primary ions. Electrode E prevents electrons from reaching the molecular beam. Charge exchange takes place in the hatched region. Between the electrodes AC_+ and AC− an acceleration field of $F = 100$, 200, 400, 1000, 2000 or 4000 V/cm is applied. After retardation by the grid R the emerging ions are energy and mass analyzed. The experiments consist of scanning the kinetic energy distribution at a fixed mass.

Typical operating parameters were: electron current 30 mA, electron energy 120 eV. At a pressure of $5\cdot10^{-4}$ Torr in the primary ionization region a primary ion current of 0.5 μA was obtained through the charge exchange region, at an ion energy of 90 eV. The energy spread was between 1.5 and 5 eV. The target gas pressure in the center of the molecular beam disc was about $5\cdot10^{-5}$ Torr. The background pressure in the apparatus resulting from primary gas effusing through the grid AC_+ amounted to 10^{-5} Torr. Great care was taken to keep the target gas background pressure in the primary ionization region as small as possible. Under the intense electron bombardment, even traces of target gas will yield considerable fragment ion intensities. Because the primary ionization region is at a more positive potential than the molecular beam region, fragments resulting from delayed decompositions can appear at and around the molecular beam potential, by virtue of an appropriate energy deficit as described above. These ions may seriously interfere with the measurement of the very small ion currents resulting from charge exchange. Efficient differential pumping of the primary ionization region is therefore extremely important.

The energy and mass selected ion current at the multiplier was, at the maximum of the beam profile, on the order of 10^{-16} A. This means an intensity loss of about two orders of magnitude compared with the earlier electron impact experiments.

IV. Possible Sources of Error

Proper operation of the apparatus was ascertained by the following tests.

a) As a check for possible collision-induced contributions to the decomposition the background pressure was raised from 10^{-5} to 10^{-4} Torr. For all processes studied (except Xe^+-benzonitrile, see below) the ratio of satellite to main peak remained constant within 1%. This remarkable insensitivity against pressure merely results from our choice of processes. In this work only decompositions were studied which have a very intense metastable peak to begin with, so that collisions, assuming reasonable cross sections, can make only minor contributions [9].

b) Possible distortion of the draw-out field by the space charge of the primary ions was checked using the process

$$Xe^+ + C_4H_4S \rightarrow C_2H_2S^+ + C_2H_2 + Xe\,.$$

Decreasing the Xe^+ current from $5 \cdot 10^{-7}$ to $5 \cdot 10^{-8}$ A did not change the satellite to main peak ratio within the error limits of $\pm 10\%$.

c) For the experiments with varying primary ion energy $e\,U_{ion}$ to be valid, the collection efficiency of the ions resulting from the charge transfer has to be independent of U_{ion}. This was ascertained for the reaction $Ar^+ + C_2H_2 \rightarrow C_2H_2^+ + Ar$ for which Maier has made reliable measurements of the cross section as a function of impact energy up to 50 eV_{LAB} [10]. In the present apparatus, the variation of the $C_2H_2^+$ yield with the Ar^+ lab energy agreed with Maier's data within $\pm 7\%$. Between 50 and 200 eV_{LAB} similarly good agreement was found for the reaction $N_2^+ + O_2 \rightarrow O_2^+ + N_2$ with the results of STEBBINGS et al. [11, 12]. This indicates that any transverse momentum transfer associated with these particular charge exchange reactions is within the range that can be accepted by our apparatus. It is a plausible assumption that the same is true for all reactions studied here, which are also exothermic (see also Sect. VII, H).

d) Finally processes other than charge exchange which also could cause dissociative ionization had to be excluded. Ionization by secondary electrons produced at the electrodes AC_+ and AC_- or ionization by the impact of the primary ions could be discarded on the basis of the observed mass spectra (see below, Tables 3 and 4). These differ radically from the usual electron impact spectra and are, moreover, characteristically different for each primary ion species. Penning-Ionization by metastable neutral particles X^* effusing from the ion source certainly occurs [13]. However, the energy available from a metastable X^* [14] is always several volts less than $RE(X^+)$, the energy liberated in charge exchange with X^+ [6]. Therefore, if the latter lies in the range of interest just above some fragmentation threshold, the former will be insufficient to produce this fragmentation.

Table 1 gives the recombination energies RE of the primary ions used. The existence of several values of RE for the same ion is a complication which, however, can often usefully be exploited (see below). A further complication concerns the identity of the primary ions. Unlike in Lindholm's work, a primary mass spectrometer could not be used for intensity reasons. This determined the choice of gases X. The mass spectra given in Table 2 show the relative abundances of the contributing ion species. The mass spectra also served to check the purity of the gases [15].

Table 1. Recombination energies RE of primary ions X^+ [a].

X^+	RE in eV (relative abundance in %)
Xe^+ [b]	12.13 (74—66); 13.44 (25—33); 12.5—16.5 (1)
Xe^{++} [c]	12.5 (15); 18—20 (85)
Kr^+ [d]	14.0 (72—50); 14.67 (27—49); 16—18 (1)
Kr^{++}	21 (almost 100)
Ar^+	15.67, 15.94 (together 99); 18—20 (1)
Ar^{++} [c]	11.5—12.5 (20); 24 (80)
Ne^+	21.56, 21.66 (together 100)
Ne^{++}	10.5—12.0 (almost 100)
He^+	24.58 (almost 100)
He^{++}	11.0—12.5 (?)
N_2^+	15.3—15.57 (almost 100)
N^+	10.97, 12.16, 14.54 (together 90); 15.03 (10)
CO^+	14.0 (almost 100)
C^+ [e]	8.58, 10.0, 11.26 (together 75—60); 12.40, 16.58 (together 24—40)
O^+ [f]	13.62 (33); 14.45, 14.98 (together 42); 16.67, 16.94, 18.64 (together 25)

[a] Most of the data are taken from E. LINDHOLM, in: Ion Molecule Reactions in the Gas Phase, Adv. in Chemistry Ser. No. 58, Amer. Chem. Soc., Washington 1966, p. 1. Data given there pertain to 100 eV electron energy and a time lapse on the order of 1 μsec after ionization. Additional Refs. see [b—f].

[b] B. TURNER, R. MATHIS, and J. RUTHERFORD, in: Proc. of the Conf. on Heavy Particle Coll. 1968, Univ. of Belfast, p. 126.

[c] W. A. CHUPKA and E. LINDHOLM, Ark. Fys. **25**, 355 [1964].

[d] J. T. SCOTT and J. B. HASTED, Advan. Mass Spectrom. **3**, 389 [1966].

[e] R. TAO, R. ROZETTI, and W. KOSKI, J. Chem. Phys. **49**, 4202 [1968].

[f] P. WILMENIUS and E. LINDHOLM, Ark. Fys. **21**, 106 [1962].

Table 2. Mass spectra of primary ions X^+ [a].

Primary gas [b, c]	primary inso relative abundance in %)
Xe	Xe^+ (77.8), Xe^{++} (16.7), Xe^{+++} (5.5)
Kr	Kr^+ (86.6), Kr^{++} (13.0), Kr^{+++} (0.5)
Ar	Ar^+ (89.6), Ar^{++} (10.4)
Ne	Ne^+ (97.5), Ne^{++} (2.5)
He	He^+ (99.9), He^{++} (0.1)
N_2	N_2^+ (65—85), N^+ (35—15), N_2^{++} (0.5—1.0)
CO	CO^+ (65—85), C^+ (18—8), O^+ (16—6), CO^{++} (0.8—1.5)

[a] Electron energy 120 eV.

[b] For the rare gases see: R. E. FOX, in: Advan. Mass Spectrom. **1**, 397 [1959]; W. BLEAKNEY, Phys. Rev. **36**, 1303 [1930]; P. T. SMITH, Phys. Rev. **46**, 773 [1936].

[c] For N_2 and CO the uncertainties of fragment ion abundance result from partial instrumental discrimination, cf. D. RAPP, P. ENGLANDER-GOLDEN, and D. BRIGLIA, J. Chem. Phys. **42**, 4081 [1965]; C. E. BERRY, Phys. Rev. **78**, 600 [1950]. In the present experiment the fragment abundance in the charge exchange region is probably in the upper part of the range given.

V. Method of Analysis

Let us consider charge exchange between an ion X^+ and a target molecule of mass m_0: $X^+ + M_0 \rightarrow X + M_0^+$, which is followed by dissociation yielding a fragment M_1^+ of mass m_1. Let the overall rate of dissociation be described by a distribution $\Pi(k)$ of individual rate constants k. Our aim is to deduce $\Pi(k)$ from the experimental data. Of course we hope to find a fairly narrow distribution $\Pi(k)$ centered around some mean k_m which we will then associate with the recombination energy $RE(X^+)$. Note that in this approach we do *not* a priory postulate the existence of some small number of discrete rate constants. With a given target gas M_0, this analysis has to be performed for each species X^+ separately.

In the earlier electron impact work, the experimental information on $\Pi(k)$ consisted mainly of the long tail that joined on to the M_1^+ peak on the energy scale towards the low-energy side. The M_0^+ peak had no tail on the low-energy side because the electron energy was chosen such that the electrons could only ionize M_0 in the beam, but not the M_0 background beyond the beam. Unfortunately, this is impossible with ion impact. The ions X^+ cannot be prevented from penetrating the beam and producing M_0^+ by charge exchange with M_0 background all the way down the draw-out field. Therefore, even the M_0^+ peak now has a low-energy tail. At any point the M_1^+ tail intensity is now the cumulative result from M_0^+ decompositions in the beam as well as in the low, but broad wings of the beam. Worse than that, the charge exchange cross section is energy dependent and changes along the tail. It is therefore impossible to obtain $\Pi(k)$ from tail measurements. Instead we based the analysis on three other kinds of data:

I. The distortion of the M_1^+ main peak shape, compared to the M_0^+ peak. This distortion, which appears as a rounding-off to the low-energy side, is really the beginning of the tail formation. It is numerically described by beam profile readings on the recorder chart at selected sampling points ΔU, $2\,\Delta U, \ldots n\,\Delta U$ along the energy axis.

II. The change in M_1^+ integral peak intensity A, as a function of draw-out field strength F. With increasing F, more and more ions M_1^+ appear at energies appreciably below the M_1^+ peak potential (i. e. in the tail), so that the absolute integral peak intensity A decreases. A was measured planimetrically. To compensate for the concomitant intensity variation due to a change in focusing conditions with changing F, all peak areas $A_{M_1^+}(F)$ were normalized to the corresponding areas $A_{M_0^+}(F)$.

III. The ratio of satellite to main peak areas, SP/MP. The satellite peak results from decompositions in the field-free region. The ions M_0^+ enter and leave this region at times τ_1 and τ_2, respectively. The difference $\tau_2 - \tau_1$ does not depend on F, as in our apparatus the ion energy in the field-free region was always kept at 570 eV. However, the larger F is, the smaller are both τ_1 and τ_2. Therefore, an increase in F leads to an increase in satellite peak intensity.

At the same time, the M_1^+ main peak decreases [see (II)]. For the evaluation of the change of SP/MP with F it is assumed that changes in focusing conditions affect SP and MP to the same extent. This is justified because of the general insensitivity of our apparatus to changes in F (the absolute intensity variation between $F = 100$ and $F = 4000$ V/cm was only a factor of 3).

For any fixed k, the measurable quantities of type (I), (II) and (III) are calculable. The contributions to them of the individual values of k are all additive, with relative weights, $\Pi(k_1)$, $\Pi(k_2), \ldots$. The experimental results of type (I), (II) or (III) can therefore be described by linear equations with $\Pi(k_i)$ as unknowns. The choice of the k_i and the total number of unknowns are arbitrary to some extent; we worked with 20 equations.

The procedure we found most satisfactory is not to rely on data of type (I), (II) or (III) alone, but rather on a mixed set of equations. For example, for the reaction of benzonitrile with Kr^+, which gives a well-developed satellite peak, 5 equations of type (III) were used, for $F = 100$, 200, 400, 1000, 2000 V/cm; furthermore 3 equations of type (II), namely for the three pairs F_1, $F_2 = 200$, 1000; 1000, 4000; 200, 4000 V/cm. The remaining 12 equations were of type (I), based on, for example, three points on the beam profile (ΔU, $2\,\Delta U$, $3\,\Delta U$), each for four values of F.

This initial step gives only the gross features of $\Pi(k)$, but over a broad range of k. In subsequent refinements different sets of 20 equations each were used which, based on the results of the first step, were chosen so as to explore the details of $\Pi(k)$ in various limited regions.

An important computational detail is the use of a least squares method described in [16]. At the expense of trebling the number of equations (i. e. we actually solved 60 equations, on an IBM 7040) it guarantees a smooth solution $\Pi(k)$.

Test runs were performed in which several known distributions $\Pi(k)$ were backcalculated. For example, with a δ-function as true $\Pi(k)$, the result of the backcalculation was a broadened peak with a full width at half maximum (FWHM) of a factor of 2.8 on the k-scale. This factor represents therefore the upper limit on the resolution of all our measurements of k.

The complete analysis in terms of $\Pi(k)$ as described above was only performed for the reactions of benzonitrile with krypton, argon, nitrogen, and carbon monoxide ions. For comparison, a much simpler analysis was also carried out for the reactions of C_6H_5CN with Kr^+ and Ar^+. In this approach the existence of two discrete values k_1, k_2 for Kr^+ and one for Ar^+ was a priori postulated. Their values [and, for Kr^+, also their relative contributions $\Pi(k_1)/\Pi(k_2)$] could then be found easily from the correspondingly simplified linear equations mentioned above. The results from the complete and simplified methods agreed quite closely (see below), so that for all other reactions only the simplified method was used.

VI. Results

In order for a decomposition to be suitable for investigation with our method, it has to meet the following requirements:

a) It should have an intense metastable peak in the usual sense (e. g. as tabulated in electron impact mass spectra [17]).

b) It has to be a decomposition of the parent ion itself. For secondary decompositions the energy content of the decomposing ion would not be accurately known because of energy fluctuation effects during the preceding dissociation [18].

c) The threshold energy of the process has to lie in the range of RE's of Table 1.

These criteria led to the processes studied in this work. Further decompositions in cyclopentane, butadiene, pyridine and H_2S were tried, but gave too little intensity or (H_2S) had too small ratios $\Delta m/m_1$.

A) Charge Exchange Mass Spectra

The fragmentation patterns of benzonitrile and benzene resulting from dissociative ionization by charge exchange were measured at the "main peak" position on the energy scale. A weak draw-out field ($F = 100$ V/cm) was employed in order to minimize effects due to the fragmentation kinetics. At $F = 100$ V/cm, the main peak comprises all fragment ions formed with a delay up to 1 μsec after the initial ionization.

The mass spectra obtained with various primary ions X^+ are given in Tables 3 and 4. The primary ion kinetic energy in the laboratory system was $U_{ion} = 20$ V, for benzene three spectra taken with $U_{ion} = 200$ V are also given.

The striking differences between charge exchange mass spectra taken with different ions X^+ are already familiar from Lindholm's work on many molecules [6]. The present two examples are shown here because, taken together with the RE's from Table 1, they provide a good qualitative insight into the fragmentation energetics. The progressing fragmentation with increasing RE is evident. Note, in par-

Table 3. Charge exchange mass spectra of Benzonitrile [a].

m/e	Primary Gas							
	Xe	Kr	CO	N_2	Ar	Ne	He	e^- [b]
103	100.0	100.0	100.0	75.0	4.2	22	12	100.0
102	1.2	0.7	0.8	3.0	2.7	6	?	1.7
77	0.5	5.9	4.1	16.6	17.8	5	1	5.8
76	1.0	29.9	19.6	100.0	100.0	—	8	32.9
75	0.3	0.5	0.6	0.5	0.4	52	64	8.3
52	0.5	0.6	0.8	1.8	0.8	15	24	5.9
51	0.5	1.0	1.0	1.2	3.0	100	73	10.3
50	1.3	0.8	1.1	1.5	0.9	100	100	18.1

[a] All intensities, uncorrected for isotopic contributions, are normalized to 100 for the most abundant fragment ion. They were recorded on the "main peak" (intersection of primary ion beam and molecular beam, see text) with a drawout field $F = 100$ V/cm and primary ion energy $e\,U_{ion} = 20$ eV; the electron energy was 120 eV.

[b] Mass spectrum for electron impact ionization (Mass Spectral Data, Amer. Petrol. Res. Inst., Res. Proj. No. 44).

Table 4. Charge exchange mass spectra of Benzene [a].

m/e	Primary Gas	Xe	Kr	Kr	CO	N_2	N_2	Ar	Ar	Ne	e^- [b]
	Uion (V)	20	20	200	20	20	200	20	200	20	
78		100.0	(100.0)	(100.0)	(100.0)	(100.0)	(100.0)	16.4	17.7	2	100.0
77		0.5	36.1	36.2	14.8	43.5	38.5	56.6	54.0	(45)	13.8
76		0.2	18.2	19.9	11.3	9.5	7.5	11.5	12.3	(13)	6.2
52		1.1	9.5	20.6	7.1	77.0	63.6	100.0	100.0	1	18.9
51		1.2	1.0	2.0	0.7	3.6	5.9	2.3	7.2	100	20.1
50		0.5	0.4	0.6	0.3	2.2	2.9	2.5	3.7	38	16.8
39		?	2.9	5.1	2.2	27.2	20.4	34.9	36.8	20	13.5

[a] For legend, see Table 3. Here data for $U_{ion}=200$ eV have been included. Some relative intensities, marked by parentheses, are at variance with results by B.-Ö. JONSSON and E. LINDHOLM, Ark. Fys. **39**, 65 [1969]. They probably contain contributions from Penning ionization (see Sect. IV, d).

[b] Mass spectrum for electron impact ionization (Mass Spectral Data. Amer. Petrol. Res. Inst., Res. Proj. No. 44).

ticular, that both in C_6H_5CN and in C_6H_6 the overall fragmentation is less with CO than with Kr. With Kr, the 33% Kr^+ in the $^2P_{1/2}$ level, RE = 14.67 eV, raises the mean RE appreciably above 14.0 eV, the RE of $Kr^+(^2P_{3/2})$, while with CO the C^+ and O^+ admixtures are of such low abundance (Table 2) that, in spite of their high RE (around 16.8 eV), the $RE(CO^+) = 14.0$ eV remains dominant.

B) Measurements of Dissociation Rate Constants

1) Benzonitrile

The rate constant distributions $\Pi(k)$ of the process $C_6H_5CN^+ \rightarrow C_6H_4^+ + HCN$ were measured using the primary ions Kr^+, Ar^+, CO^+ (accompanied by C^+ and O^+) and N_2^+ (with N^+) to produce $C_6H_5CN^+$ by charge exchange. Fragmentation by collision with Xe^+ was also observed, but appears to be an endothermic process (see below). As a qualitative illustration, Fig. 3 shows the M_0^+ beam profile, in this case for $X^+ = CO^+$ impact, and the various M_1^+ beam profiles. The steadily increasing distortion in going from Ar^+ to Kr^+ is obvious. It must be emphasized that the final results are derived from many runs under varying conditions and are therefore much more accurate than an individual example such as in Fig. 3 would seem to warrant. The Ar^+, N_2^+ and CO^+ curves in Fig. 3 are all rather similar. Nevertheless, the corresponding satellite peaks have very different intensity; the ratio of satellite to main peak (at $F = 100$ V/cm, $U_{ion} = 90$ V) is in the order Kr^+, CO^+, N_2^+, Ar^+: SP/MP $= 0.47$; 0.24; 0.028; < 0.003. This indicates components of $\Pi(k)$ at low k for the first two reactions, which are almost absent for the third and completely missing for the fourth.

These qualitative expectations are borne out by detailed analysis. Each curve of the type shown in Fig. 3 was scanned at least 10 times and averaged. The entire amount of experimental data gathered for charge exchange between benzonitrile and any one primary ion species X^+ was simultaneously processed by the analytical method described above. It yielded automatically the complete rate constant distribution $\Pi(k)$ for each X^+ species between about $k = 5 \cdot 10^4$ and 10^9 sec^{-1}.

The resulting four distributions $\Pi(k)$ for X = Kr, CO, N_2 and Ar are given in Figure 4. They differ dramatically in shape. Moreover, their structure can be closely correlated with the RE's in Table 1: Each RE is represented by a peak in $\Pi(k)$, whose location on the k-axis is a monotonic function of RE (cf. the peak labeling in Figure 4).

The three peaks in Fig. 4 a can be attributed to three different ionic species. The big CO^+ peak at low k explains the previously mentioned satellite peak for this reaction. In Fig. 4 b the two peaks are due to the $^2P_{3/2}$ and $^2P_{1/2}$ states of Kr^+. In Fig. 4 d, the same two states of Ar^+ are not resolved. Note the position of the Ar^+ peak on the k-axis: in contrast to the Kr^+ peak, it covers the range of large k only, which explains the absence of a satellite peak in the Ar^+ experiments. In Fig. 4 c the N_2^+ peak is again composite. It comprises several values of k, corresonding to recombination of N_2^+ into $N_2 X^1 \Sigma^+$ ($v' = 1$ and $v' = 0$).

The desired dependence $k(E)$ can now be obtained by combining Figs. 4 a – d into one figure.

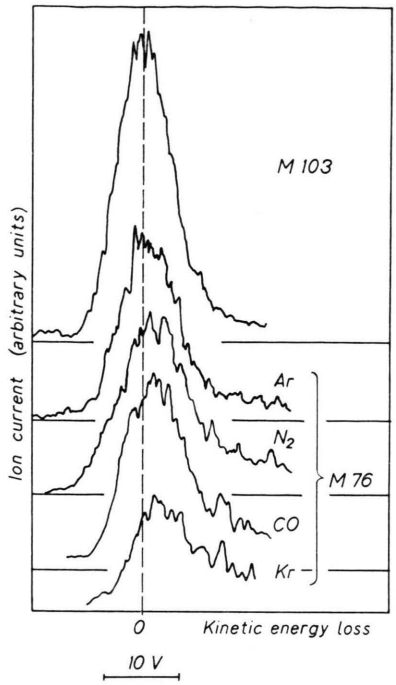

Fig. 3. Typical results for $C_6H_5CN+X^+ \rightarrow C_6H_5CN^+ + X$ (top trace) and $C_6H_5CN+X^+ \rightarrow C_6H_4^+ + HCN + X$ (with X^+ = sum of all ions formed from CO in top trace and from Ar, N_2, CO, Kr in the lower traces). Draw-out field $F = 1000$ V/cm. Compare the schematic Fig. 1: The progressing peak distortion indicates an increase of mean parent ion lifetime. Satellite peaks are not shown.

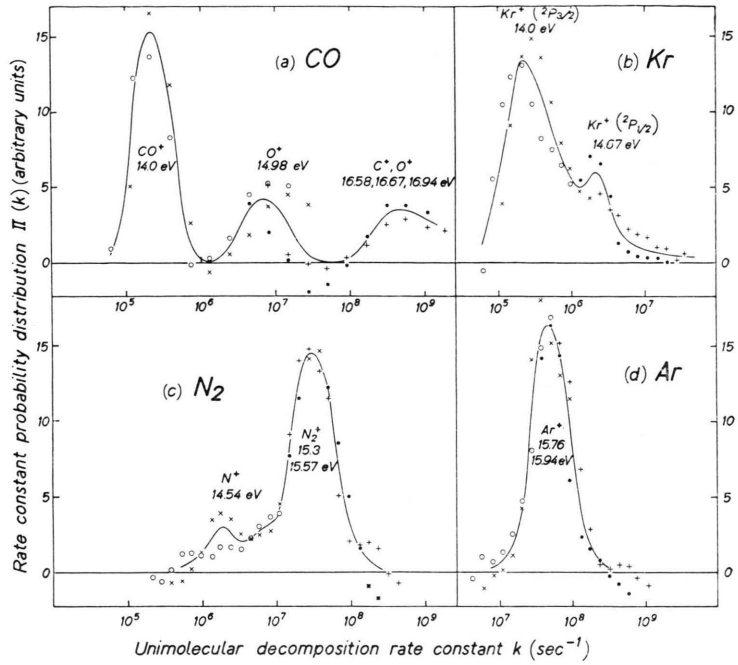

Fig. 4. Probability distributions $\Pi(k)$ of rate constants k for unimolecular decomposition of $C_6H_5CN^+$, produced by charge exchange with ions from four different primary gases. $\Pi(k)$ was obtained from curves like those shown in Fig. 3 by a mathematical procedure explained in the text. The pairs of symbols (○, x) and (●, +) give a measure of the uncertainty of the calculation; for ○ and ● the set of selected values k_i (see Sect. V) was displaced as a whole towards lower k, as compared to x and + by a factor of 2. Negative values of $\Pi(k)$ are also a computational artifact.

As a prerequisite, the zero point on the E-scale has to be fixed. According to the principle of charge exchange ionization, $E = \mathrm{RE} - \mathrm{I.P.} + \Delta E$, where I.P. = adiabatic ionization potential of benzonitrile. ΔE represents the sum of the initial average thermal energy and the average energy transferred in the collision. The former is estimated to be about 0.1 eV (taken over from butane[19], which has a similar number of degrees of freedom). The latter can be assessed by observing the effect of a *change* of the bombarding ion energy $e\,U_{\mathrm{ion}}$ in our experiment. Results presented below lead to a value of about 0.15 eV. Thus ΔE is taken as 0.25 eV.

In Fig. 5 the positions of all maxima of the four distributions $\Pi(k)$ from Fig. 4 a – d are plotted

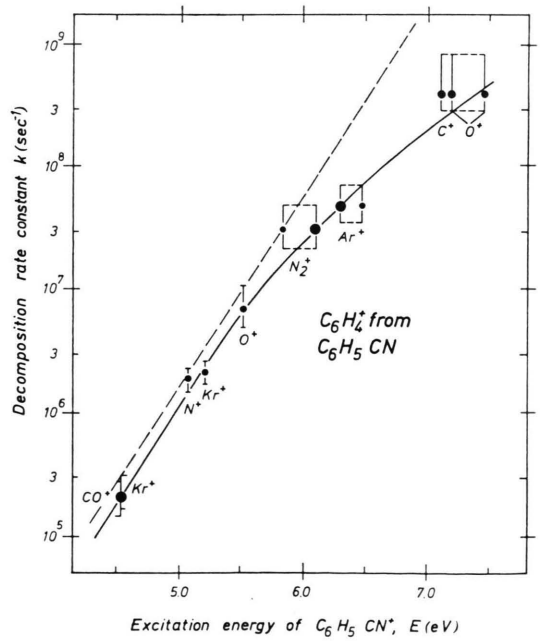

Fig. 5. Dependence of unimolecular decomposition rate constant k on internal energy E of $C_6H_5CN^+$. The solid curve was obtained by plotting the peak positions from Fig. 4 versus $E = \mathrm{RE} - \mathrm{I.P.} + 0.25$ eV (see text). The dashed curve gives $k(E)$ as obtained from earlier experiments with electron impact ionization.

versus E, which was calculated using I.P. = 9.705 eV [20] and the RE's from Table 1. The smooth variation of $\log k$ with E which is obtained is extremely gratifying. It gives strong support to our procedure of analysis and to the thesis that this curve truly represents the function $k(E)$.

The error bars in Fig. 5 indicate the 90% width of the $\Pi(k)$ peaks. This was preferred to FWHM because of the incomplete peak resolution in Fig. 4 b and 4 c. Where several RE contribute to the same peak (N_2^+, Ar^+, C^+/O^+), the presumably predominant component is marked with a heavier dot.

Charge exchange with Xe^+ also gave a measurable satellite peak. It would, by extrapolation, correspond to a point at $k = 3 \cdot 10^4\ \mathrm{sec}^{-1}$, RE = 13.4 eV. However, this point was not included in Fig. 5 because the process

$$Xe^+ + C_6H_5CN \rightarrow C_6H_4^+ + HCN + Xe$$

is most likely endothermic. This follows from the appearance potential of $C_6H_4^+$ of 13.9 eV [21]. More convincing, in view of the uncertainties of all appearance potential measurements, is the unusual dependence of the satellite peak intensity [22] on the primary ion kinetic energy $e\,U_{\mathrm{ion}}$. Compared to the "ordinary" increase of intensity towards lower U_{ion} which was observed in several other cases (see Sect. VI, C2), the rise was here 4 times steeper. This suggests transverse momentum transfer leading to ion loss at large U_{ion} (see [23]). The intensity of $C_6H_5CN^+$ from charge exchange with Xe^+ was very much lower than with the other gases X. This also points to a different mechanism, i. e. an endothermic process.

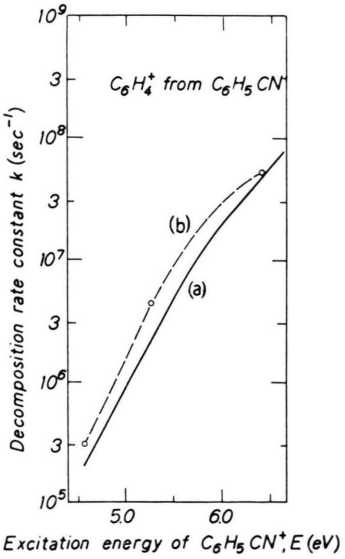

Fig. 6. Comparison of $k(E)$ for $C_6H_5CN^+ \rightarrow C_6H_4^+ + HCN$ as obtained by the complete (solid curve) and a simplified (dashed curve) mathematical procedure.

The well-established $k(E)$ for the benzonitrile decomposition was used as a test for the simplified method of analysis which presupposes discrete values of k_{m} (see above). The result for $k_{\mathrm{m}}(E)$, deduced from experiments with Kr^+ and Ar^+ only, is compared in Fig. 6 with the more accurate $k(E)$ from Figure 5. The good agreement obtained was taken as justification to use only the simplified method for the determination of $k(E)$ of benzene and thiophene.

2) Benzene

Of the four important primary decompositions $C_6H_6^+ \rightarrow C_6H_5^+$, $C_6H_4^+$, $C_4H_4^+$ and $C_3H_3^+$ only the first and third could be used to derive a $k_{\mathrm{m}}(E)$. The second and fourth were masked by background on mass 76^+ (benzonitrile residue) and 39^+ (K^+ from surfaces), qualitatively they appeared to behave similarly to the first and third process, respectively. The function $k_{\mathrm{m}}(E)$ for $C_6H_6^+ \rightarrow C_4H_4^+$, as determined from charge exchange with Kr^+, is given in Figure 7. It is seen that the two Kr^+ states yield two widely different k_{m}. Ar^+ with its relatively high RE gave already a practically undistorted peak, so that here only a lower limit for k_{m} could be stated.

The important process $C_6H_6^+ \rightarrow C_6H_5^+$ presented special difficulties. The energy deficit associated with the delayed loss of one mass unit is very small. Consequently peak distortion and tail are negligible. The only measurable quantity is the satellite peak, which is here located very close to the main peak. It is extremely intense, as is shown in Fig. 8 a and b. From its intensity (relative to the main peak) the $k_{\mathrm{m}}(E)$ for this process, as given in Fig. 7, was derived as follows. For Ar^+ a common k value was attributed to the two RE's of 15.76 and 15.94 eV. This k_{m} can then be calculated immediately from the experimental SP/MP ratio. For Kr^+ two values of k (at 14.0 and 14.7 eV) combine to give the observed SP/MP ratio. From this experiment alone $k_{14.0}$ and $k_{14.7}$ can only be determined if one makes an assumption about

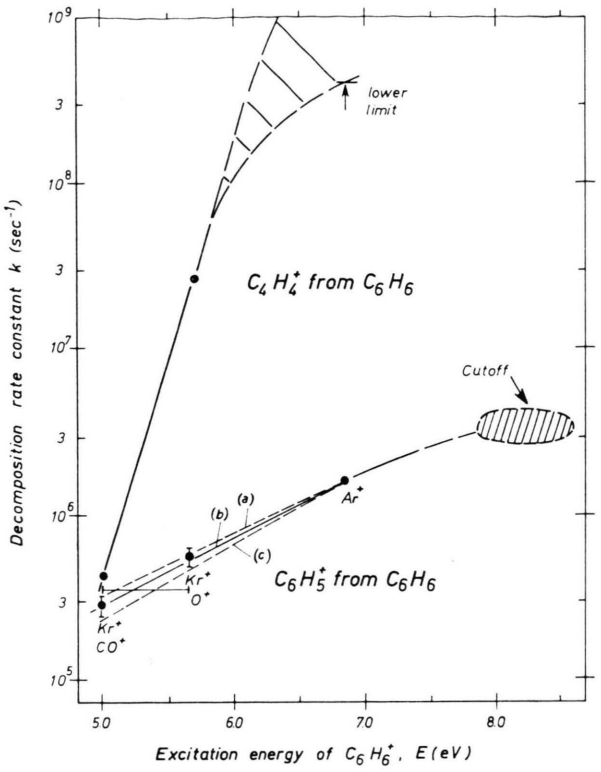

Fig. 7. Dependence of unimolecular decomposition rate constant k on internal energy E of $C_6H_6^+$, for two different decomposition paths. The curves a, b, c are for three assumed ratios of the charge exchange cross sections for $Kr^+(^2P_{3/2})+C_6H_6$ and $Kr^+(^2P_{1/2})+C_6H_6$, respectively (see text). Boundary values for this $k(E)$ curve are given by the horizontal bar. Two further points as well as the area "Cuotff" (see Sect. VII, E) all support the exceedingly slow rise of this $k(E)$. The contrasting steep rise of $k(E)$ for $C_4H_4^+$ formation proves that the two processes are not in competition with each other.

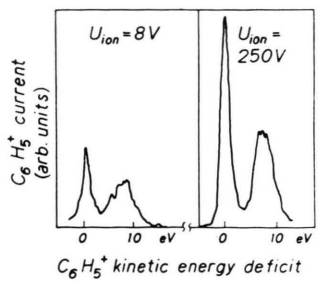

Fig. 8. Main peak (on the left in each scan) and satellite peak of the process $C_6H_6^+ \rightarrow C_6H_5^+ + H$, for two different kinetic energies $e\,U_{ion}$ of the primary ions (in this case CO^+). The comparatively small increase of the main peak: satellite peak intensity ratio with increasing U_{ion} demonstrates the inefficient conversion of kinetic into internal energy.

the associated relative charge transfer cross sections, $Q_{14.0}$ and $Q_{14.7}$. Furthermore, $k_{14.0}$ and $k_{14.7}$ were required to fulfill the condition that, together with the k value for Ar^+, they lie on a straight line in a $\log k(E)$ plot [24]. The resulting functions $k(E)$ are shown in Fig. 7 for the assumed ratios $Q_{14.0}/Q_{14.7} = 3.0$; 1.0; 0.33 (curves a, b, c respectively) [25]. The value of k for the limiting, but quite unlikely cases $Q_{14.0} = 0$ or $Q_{14.7} = 0$, $k = 3.6 \cdot 10^5$ sec^{-1}, is also shown.

An alternative method of finding $k_{14.0}$ and $k_{14.7}$ was also used. Instead of the assumptions about $Q_{14.0}/Q_{14.7}$ and the straight line conditions, the experimental data from CO^+ charge exchange were adduced. The rather involved analysis [26] yielded points also shown in Fig. 7, in good agreement with the first method.

The $k(E)$ obtained in this way is also in accord with the SP/MP ratio measured with N_2^+ (and N^+) primary ions.

3) Thiophene

The primary decomposition $C_4H_4S^+ \rightarrow C_2H_2S^+ + C_2H_2$ occurred with a measurable delay only after charge exchange with Xe^+. Xe^+ has RE's of 12.13 and 13.44 eV. The simplified method of analysis, as described above, yielded corresponding values of k differing by 2.4 orders of magnitude. Between these, $k(E)$ was interpolated as shown in Figure 9.

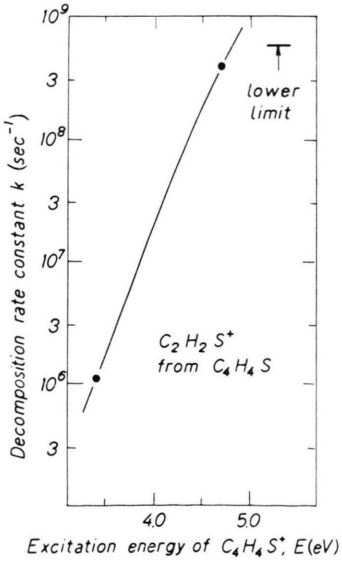

Fig. 9. Dependence of unimolecular decomposition rate constant k on internal energy E of $C_4H_4S^+$, obtained by the "simplified" procedure from charge exchange with Xe^+ ions.

C) Charge Exchange at varying Ion Impact Energy

1) Translational Energy Transfer

All experiments discussed so far were done with 90 eV primary ions. By varying the ion impact energy the amount of energy transferred from kinetic to excitation energy can be measured.

The ratio SP/MP is a sensitive indicator for the amount of energy transferred. A spectacular qualitative example is given in Figure 8. Here the kinetic energy in the c.m. system changes by a factor of 30, from 0.6 to 18 times the recombination energy. The ratio SP/MP, however, only changes by a factor of 1.4. Therefore the amount of kinetic energy transferred in this charge exchange collision is very small. This is true in all cases studied. Figure 10 gives two other examples. Since the kinetic energy plays only such a minor role, the curves $k(E)$ obtained above (with $U_{\text{ion}} = 90$ eV) can now serve as gauges to measure quantitatively the amount of translational energy transfer.

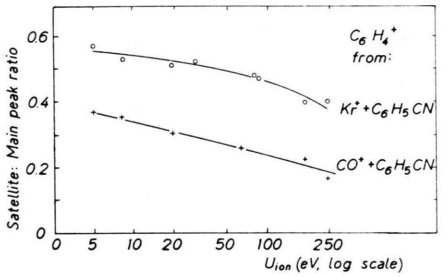

Fig. 10. Variation of the intensity ratio satellite peak : main peak with U_{ion} (see Fig. 8) ($F = 100$ V/cm).

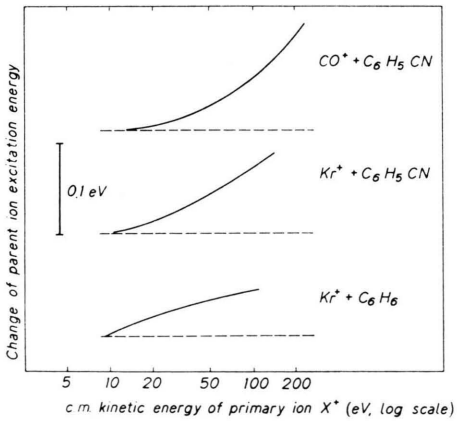

Fig. 11. Kinetic to internal energy transfer for three charge exchange processes, obtained from data such as in Fig. 10 via the $k(E)$ curves of Figs. 5 and 7.

Measurements were made for ion energies $e\,U_{\text{ion}}$ between 8 and 250 eV (LAB system). The ratio SP/MP of satellite to main peak intensity was determined for different field strengths F. The results for each energy $e\,U_{\text{ion}}$ were analyzed as above (using the "simplified method") and yielded values of k which, at each RE, increased monotonically with U_{ion}. This variation of k was converted via the known $k(E)$ to yield the change of internal energy E. The result is shown in Figure 11. It can be seen that less than 0.1% of the c.m. kinetic energy is transferred in these charge exchange processes.

2) Charge Exchange Cross Section

The relative cross section, as a function of U_{ion}, for formation of a secondary ion by charge exchange cannot, in general, be obtained directly from a measurement of the main peak intensity as a function of U_{ion}. The reason is the transfer of kinetic into excitation energy as discussed in Sect. VI, C1, which causes k and hence the fraction of the total ion yield collected within the peak to change with U_{ion}. Among the cases studied, this effect was negligible only for

$$C_6H_5CN + Ar^+ \rightarrow C_6H_4^+ + HCN + Ar\,,$$

because here k is so large (see Figs. 4 and 5) that a small variation is insignificant. The main peak intensity for this process, normalized to the Ar^+ current, is shown in Fig. 12 [curve (d)].

For Kr^+ the main peak intensity, normalized to the primary ion current, was corrected to obtain the true relative cross section $Q(U_{\text{ion}})$ using the results of Sect. C1. In that analysis, for each U_{ion} both $k(\text{RE} = 14.0)$ and $k(\text{RE} = 14.67)$ as well as their relative contributions were obtained. This information was used here to convert the main peak intensity at mass 76 into the total ion yield, $I_{76^+}(U_{\text{ion}})$. The two contributions from $Kr^+(^2P_{1/2})$ and $Kr^+(^2P_{3/2})$, $I_{76^+}{}^{(1/2)}(U_{\text{ion}})$ and $I_{76^+}{}^{(3/2)}(U_{\text{ion}})$, were obtained separately, see Fig. 12, curves (b) and (c). The main peak intensity raw data [curve (a)] are also given. A comparison of curves (b) and (c) with (a) illustrates the effect of the correction for the k variation [27]. Figure 13 shows the analogous curves for charge exchange of Kr^+ with benzene, forming mass 52 ions; curve (a) is the uncorrected main peak intensity, curve (b) and (c) give the true $Q(U_{\text{ion}})$ for the $Kr^+(^2P_{1/2})$ and $Kr^+(^2P_{3/2})$ species, respectively.

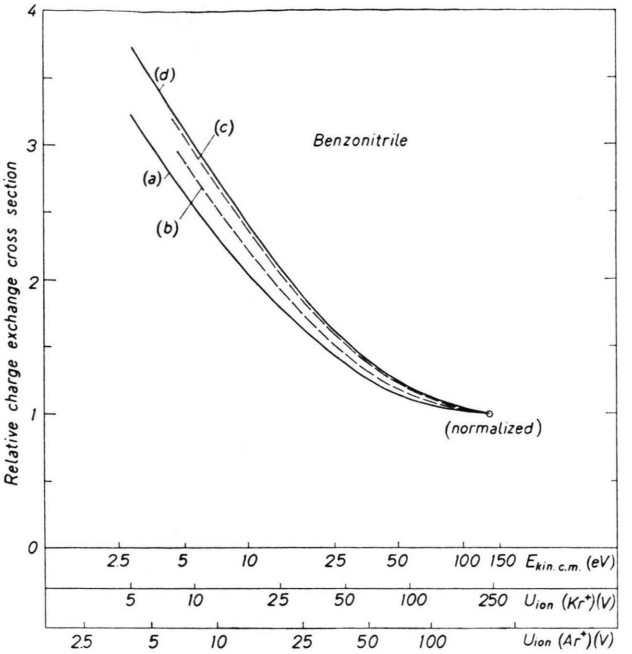

Fig. 12. Dependence of dissociative charge exchange cross section on relative kinetic energy, for $Kr^+ + C_6H_5CN \rightarrow C_6H_4^+ + HCN + Kr$ (curves a–c) and $Ar^+ + C_6H_5CN \rightarrow C_6H_4^+ + HCN + Ar$ (curve d); (a) gives the uncorrected normalized main peak intensity, (b) and (c) the true separate contributions, as derived from (a), from $Kr^+(^2P_{1/2})$ and $Kr^+(^2P_{3/2})$, respectively. Unlike (a), the normalized main peak data of curve (d) need not be corrected for kinetic effects.

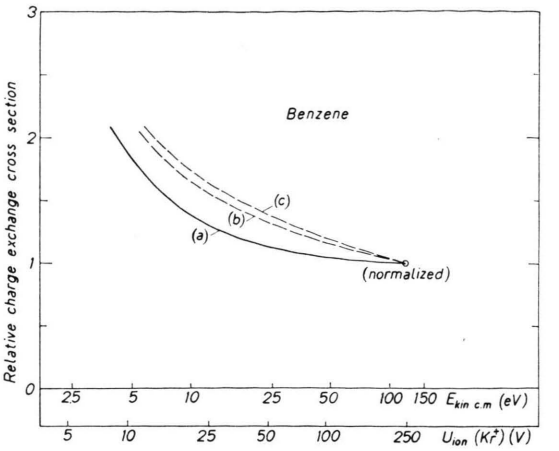

Fig. 13. Dependence of dissociative charge exchange cross section on relative kinetic energy, for $Kr^+ + C_6H_6^+ \rightarrow C_4H_4^+ + C_2H_2 + Kr$. See Figure 12.

VII. Discussion

A) Is the decay law for $C_6H_5CN^+ \rightarrow C_6H_4^+ + HCN$ *an exponential?*

The benzonitrile ion now is the first system whose decomposition behaviour is known in considerable detail. Previous studies of unimolecular decompositions gave only average rate constants k or at best indicated some structure or changes in the broad distributions $\Pi(k)$ [1, 5]. The results depicted in Fig. 4 show that in the present experiment benzonitrile ions were prepared in states with narrow distributions $\Pi(k)$.

These distributions are remarkably sharply peaked, considering the various factors contributing to their width:

a) The limited resolution of the unfolding process, resulting in an uncertainty of a factor of 2.8 on the k-scale;

b) the broadening from experimental noise;

c) the spread of thermal energy (0.1 eV, corresponding to an uncertainty of k within a factor of 1.4, cf. Fig. 5);

d) the spread of RE's (0.16 eV for Ar^+, 0.29 eV for N_2^+, corresponding to k values differing by a factor of 1.8 and 2.8, respectively).

e) The spread of energy transferred from kinetic energy.

The observed widths (FWHM) of the $\Pi(k)$ peaks are a factor of 4 for Ar^+ and a factor of 5 for N_2^+. Thus the true $\Pi(k)$ may well be a δ-function for each RE; a generously estimated upper limit to its width is a factor of 2.

MIES and KRAUS [28] as well as BUNKER [29] have discussed the possibility of non-exponential unimolecular decay. Bunker performed classical trajectory calculations on molecules dissociating after collisional activation in a heat bath. This is appropriate to the usual chemical unimolecular decomposition, but less so to the present, rather specific mode of excitation. Mies and Krauss considered individual quantum mechanical resonance states (corresponding to the activated ion states) with overlapping level widths. It was shown that departures from exponential decay can occur through the interaction of the resonance states with the dissociation continuum.

If a non-exponential decay existed, it would in our experiment show up as a more or less broadened distribution $\Pi(k)$. We conclude, therefore, that in the present cases the conditions for non-exponential decay (specified in [28] in terms of level width

and spacing distributions, in [29] in terms of hindrance of intramolecular energy flow) probably do not obtain. In particular, Mies and Krauss point out the possibility that metastable (i. e. long-lived) ions with excitation energies well above the dissociation threshold may exist. For benzonitrile, Fig. 5 shows clearly that the lifetime is monotonically shortened as the excitation energy increases.

B) Comparison with $k(E)$ from electron impact experiments

The earlier electron impact work [4] also gave the dependence $k(E)$ for $C_6H_5CN^+ \rightarrow C_6H_4^+ + HCN$, though only with some assumptions on the density of states and the threshold law for excitation of each state. Justification of these assumptions was at that time given by the excellent agreement of calculated and measured ion yield, as a function of electron energy for "normal" and "metastable" fragment ions. The $k(E)$ obtained in that work was a linear dependence of ${}_{10}\log k$ on E with slope 1.54/eV [30]. This function is shown in Fig. 5 by the dashed line. The position on the E-axis was fixed by means of the measured appearance potential of the "normal" fragment $C_6H_4^+$, $AP(76^+) = 15.2 \pm 0.2$ eV [4, 21]. "Normal" fragments in our apparatus are those with $k \gtrsim 10^7\ \mathrm{sec}^{-1}$. Therefore the dashed line in Fig. 5 is positioned such that $k = 10^7$ is reached at $E = 15.2 - 9.705 + 0.1 = 5.6$ eV (9.705 eV = I.P. of benzonitrile [20], 0.1 eV = average thermal excitation energy). It is seen that the functions $k(E)$ as obtained from electron impact and charge exchange are in excellent agreement in the lower part. At high k, the latter curve is certainly more reliable. The deviation of the former curve is not unexpected in view of the assumptions made in its derivation.

The reassuring agreement between both sets of data also lends strong support to the $k(E)$ curves for butane and heptane derived from electron impact experiments [5]. In those cases the same assumptions as for benzonitrile were made, though under somewhat less favourable circumstances. Unfortunately, a check with the present method is impossible because of the lack of suitable charge exchange partners.

C) The concurrent reaction $C_6H_5CN^+ \rightarrow C_6H_5^+ + CN$

According to the mas spectrum (Table 3), the mass 77 intensity is only about 15 – 20% of the 76^+ intensity, for Kr^+ through Ar^+. Correction for the $^{13}C^{12}C_5H_4^+$ contribution reduces it further by a factor of about 0.6. With this low abundance and the $^{13}C^{12}C_5H_4^+$ background it was not possible to measure $k(E)$ directly in the same way as for mass 76. This is unfortunate since such a measurement would have resolved unambiguously the problem of whether the losses of CN and HCN from the benzonitrile ion are in competition with one another or not. In the first case, which conforms to the usual ideas of the QET, at each RE the value of k measured for the two processes would have been exactly the same, namely equal to the overall decomposition rate of the parent ion. The ion yields measured at mass 76 and mass 77 would in this case have been in the ratio k_{76}/k_{77}, with $k = k_{77} + k_{76}$. (Note that in this case k_{76} and k_{77} cannot be measured directly, but only inferred from the relative ion yields and the value of k.) The ratio k_{76}/k_{77} could, of course, have been different for each RE. For the case of isolated, non-competing decompositions to form 76^+ and 77^+ ions, one would in general at each RE measure different values of k for the two fragments. Also, these would not be related to the relative ion yields.

We adopt the assumption of competing processes as the more likely one. This means that the $k(E)$ given in Fig. 5 is to be interpreted as $k_{77} + k_{76}$. k_{76} alone would be about 10% smaller at all energies, k_{77} would be smaller by a factor of 10. If, on the other hand, the mass 77 formation is not in competition with mass 76 formation, Fig. 5 gives the true k_{76} (which is thus not very sensitive as to which of the two assumptions is made), and k_{77} is then completely unknown.

D) Two clearly non-competing decompositions of $C_6H_6^+$

The two concurrent decomposition paths of $C_6H_6^+$, leading to $C_6H_5^+$ and $C_4H_4^+$, respectively, constitute a clear-cut example of the existence of reactions that are not in competition with one another. Here, in contrast to the two $C_6H_5CN^+$ decompositions discussed in the preceding paragraph, we did measure separately the rate constants for

the two decomposition paths. Figure 8 shows that for them the functions $k(E)$ are completely different. It is to be emphasized that at each RE the two values of k were obtained quite independently. For example, with Ar^+ as primary ion the mass 52 main peak was identical in shape to the mass 78 main peak, indicating an unmeasurably large $k_{78^+ \to 52^+}$, while at mass 77 a considerable main peak distortion and a satellite peak were observed, leading to $k_{78^+ \to 77^+} = 1.56 \cdot 10^6\,\mathrm{sec}^{-1}$. For competing reactions, the fast $78^+ \to 52^+$ process would have suppressed any slow mass 77 formation. Thus, Fig. 8 does not simply mean that a fast and a slow decomposition of $C_6H_6^+$ exist side by side (which would, of course, be entirely compatible with the QET), but gives proof, because of the principle of our measurement, that these processes are non-competing.

The same seems to be true for the pair of processes $C_6H_6^+ \to C_3H_3^+ + C_3H_3$ [steep $k(E)$] and $C_6H_6^+ \to C_6H_4^+ + H_2$ [slow $k(E)$ rise], which unfortunately could not be measured accurately (see above). Thus, it seems that processes involving breakage of a C – C bond and those involving hydrogen loss originate from different types of excited states, between which energy randomization is not possible within the time ($\approx 10^{-6}$ sec) available for decay [31].

E) Comparison of $k(E)$ for $C_6H_6^+ \to C_6H_5^+ + H$ with electron impact metastables

The uncertainties of the $k(E)$ for 77^+, resulting from the complications with the two RE values of Kr^+, cannot possibly invalidate the above conclusion. Furthermore, there is additional support for this $k(E)$ from a comparison with the electron impact experiments. In those experiments (see, e. g. Fig. 1 in [32]) large satellite:main peak intensity ratios were found. They can be predicted by an extrapolation of $k(E)$ for 77^+ in Figure 7. The lower part of $k(E)$ will produce the satellite peak, while the upper part contributes predominantly to the main peak. The extrapolation has to be terminated at the onset of the first secondary dicomposition, presumably $C_6H_5^+ \to C_4H_3^+ + C_2H_2$. The appearance potential of $C_4H_3^+$ is 17.6 ± 0.1 eV [33]. Also, the distribution $P(E)$ of the states excited by 70 eV electrons and leading to $C_6H_5^+$ formation has to be known. For lack of electron impact data, a rough estimate for $P(E)$ for the present charge exchange excitation was used; $P(E)$ seems to drop by a factor of about 2 between 14 and 17 eV [26]. With this $P(E)$ the SP/MP ratio measured with electron impact is obtained, if $k(E)$ in Fig. 7 is extrapolated such that $k = 3 \cdot 10^6\,\mathrm{sec}^{-1}$ at the "cutoff" energy of 17.6 eV [34].

Thus an additional, though rather uncertain "point" of $k(E)$ for $C_6H_6^+ \to C_6H_5^+ + H$ is obtained. It again supports the extraordinarily slow rise of this function: Over an E-interval of 3 eV $k(E)$ increases by only one order of magnitude. This unusual behavior of the simplest of all $C_6H_6^+$ dissociations can certainly not be explained by the unmodified QET. Its elucidation, probably in terms of forbidden transitions between electronic states, remains an interesting problem.

F) Appearance potentials

JONSSON and LINDHOLM have recently measured the breakdown diagram of benzene with charge exchange [35]. From it they obtained appearance potentials for $C_6H_5^+$ and $C_4H_4^+$ ions. The former one, 13.8 eV, agrees well with our $k(E)$ in Fig. 7; it is also in agreement with a value from photoionization, 13.8 ± 0.2 eV [36]. For $C_4H_4^+$ the lowest appearance potential reported for electron impact is 14.5 ± 0.2 eV [33]. Jonsson and Lindholm find about 14.0 eV, by a somewhat uncertain extrapolation. From our $k(E)$ it appears that an even lower value, about the same as for $C_6H_5^+$ (13.8 ± 0.2 eV), might be better still [37]. In 1963, ROSENSTOCK and KRAUSS [38] cited the large differences between the appearance potentials of various fragments formed from $C_6H_6^+$ as evidence for dissociation paths without effective competition. For the case of $C_6H_5^+/C_4H_4^+$ this argument has now been invalidated by the similar onsets of the corresponding $k(E)$ curves. However, ironically, the conclusion remains unaltered by virtue of the different slopes of these very same curves.

G) Kinetic energy transfer

A fundamental problem with charge exchange processes $X^+ + A \to A^+ + X$ is the question of how much kinetic energy is transferred from the X^+ ions into excitation energy of A^+. Only if this energy transfer is negligible has the excitation energy E_i of A^+ the well-defined value

$$E_i = \mathrm{RE}(X^+) - \mathrm{I.P.}(A) + E_{th}(A)$$

(cf. abscissa of Fig. 5). Lindholm's experiments were designed so as to circumvent this problem [6]: By extracting the ions A^+ at right angles ("perpendicular geometry") to the X^+ beam, only those ions A^+ should be *observed* which are formed with little or no transfer of kinetic energy. By the same token, though, Lindholm cannot make any statement about the extent to which kinetic energy can be transformed into excitation energy.

In fact it is known from experiments with the "longitudinal" type of apparatus, where X^+ and A^+ ions have parallel paths (like in our instrument) that the kinetic energy of X^+ can be converted into electronic energy of A^+. An example is the endothermic process $Kr^+ + D_2 \rightarrow D_2^+ + Kr$ [10]. Because the reaction $Kr^+ + H_2 \rightarrow H_2^+ + Kr$ has been found by GUSTAFSSON and LINDHOLM [39] to occur with large cross section, Maier argues that in this case the perpendicular geometry employed in [39] cannot have discriminated effectively against detection of the H_2^+ product. Nevertheless, the general success of Lindholm's numerous measurements of ionic breakdown patterns, which are all based on the assumption of monoenergetic excitation by charge exchange, lends strong support to his method.

The majority of Lindholm's investigations were concerned with exothermic reactions, like ours. For these the above relation for E_i may well be fulfilled in spite of incomplete discrimination against processes with momentum transfer. Exothermic charge exchange of X^+ with a complex molecule A will usually be nearly resonant with some excited level of A^+. Near-resonant charge exchange is expected to occur with a large cross section [40], so that glancing collisions will predominate which transfer very little momentum and kinetic energy.

Accurate measurements of the extent of kinetic to excitation energy transfer are thus highly desirable in order to assess the importance of the discrimination effect of the perpendicular geometry.

The occurrence of some kinetic energy transfer even for exothermic reactions with complex molecules may be inferred from the variation of charge exchange mass spectra with the X^+ kinetic energy $e\,U_{ion}$ [35, 41, 42]. If the energy content of an ion A^+ is changed by some amount δE, the branching ratio of its decomposition products B_1^+, B_2^+, ..., i. e. the mass spectrum, will also change. However, a quantitative evaluation of δE as a function of U_{ion} is extremely difficult. It would require not only detailed knowledge of the decomposition kinetics but also of the discrimination characteristics of the apparatus. In fact, longitudinal and perpendicular instruments can give quite dissimilar mass spectra, depending on U_{ion} [6]. Our measurements of δE (see Sect. VI, C1) is also based on the evaluation of kinetic effects, but in a straightfordward manner. Also, as was shown in Sect. IV c, our data are insensitive to transfer of transverse momentum. This is particularly true for the present problem of kinetic energy transfer: The results of Sect. VI C1 are derived from measurements of the satellite peak to main peak ratio, as a function of U_{ion}. Should there be some ion los due to transverse momentum transfer, it would affect both peaks similarly and would cancel out in their intensity ratio.

The results presented in Fig. 11 appear to be the first data of this kind. The very small increase of internal excitation energy with a large variation in relative translational energy is consistent with the picture of near-resonant, large impact parameter collisions.

This finding at the same time supports the value of the recombination energies RE assumed in this work (Table 1), which were derived by Lindholm from spectroscopic data. As he has pointed out [6], in very close collisions the optical selection rules would break down, and different RE's would obtain.

GURNEE and MAGEE have treated near-resonant charge exchange processes semi-quantitatively [43]. In their calculation, using the impact parameter method, they compute the probability for near-resonant charge transfer, relative to the case of exact resonance, as a function of the energy deficit ε. Their result is a Gauss function, centered around $\varepsilon = 0$ (i. e. exact resonance), whose width increases with the relative velocity v (see [43], Fig. 9). Another parameter entering into the width is the screening factor of the Slater type wave functions used, which was chosen rather arbitrarily.

In our experiment, for $Kr^+ + C_6H_5CN$, the relative velocities range from $v = 6.5 \cdot 10^5$ cm/sec to $2.5 \cdot 10^6$ cm/sec. According to [43], at our lowest velocity only $C_6H_5CN^+$ states in very close resonance with $RE(Kr^+)$ could be excited (within about 0.02 eV), whereas for the highest velocity states lying up to about 0.15 eV off resonance would be accessible. The sign of ε does not enter, so that the excited energy band widens up symmetrically around

exact resonance as the impact velocity is increased. However, for large molecules the density of states increases very rapidly with energy [44–46], so that the net result will be an upward shift of the mean excitation energy of $C_6H_5CN^+$. We believe, therefore, that our results shown in Fig. 11 can, as far as the order of magnitude is concerned, be explained by the theory of Gurnee and Magee. A quantitative comparison would require an adaptation of their calculation to our specific cases as well as a calculation of the density distribution of excited states of the organic ions around the RE values in question.

H) Charge exchange cross section

In Figs. 12 and 13 we find a decrease of the cross section for our particular dissociative charge transfer processes bc a factor of 3 in going from about 5 to 150 $V_{c.m.}$. This is more than the variation calculated by GURNEE and MAGEE [43], which, over the same energy interval, amounts to a decrease by about 1/3 for atomic and a factor of 2 for diatomic systems. The corresponding experiments [40] also show this slower fall-off. However, we believe it unlikely that our steep decrease is an artifact caused by transverse momentum transfer (see IV, c). This is supported by the fact that the cross sections for charge exchange of Ar^+, Kr^+ and CO^+ with C_6H_5CN fall off in a very similar manner, despite the differing masses of the reactant ions. Thus, charge exchange with aromatic molecules really seems to depend more strongly on the relative velocity than with smaller systems. A rough measure of the relative cross sections, at a fixed impact energy, of various ions X^+ can be obtained from the $\Pi(k)$ distributions in Fig. 4 by dividing the relative peak heights by the relative abundances in the ion beam. For example the ratio of the peak heights at RE = 14.0 and RE = 14.7 in Fig. 4 is $2.2 \pm 20\%$. The intensity ratio of $Kr^+(^2P_{3/2}) : Kr^+(^2P_{1/2})$ is probably 2 : 1 (see [6]), which indicates a similar cross section for the two species in agreement with Fig. 12.

I) Double ionization by charge exchange

As a product of charge exchange between H^+ and benzonitrile the ion $C_6H_5CN^{++}$ ($m/e = 51.5$) was observed. It is attributed to autoionization of an intermediary $C_6H_5CN^+$. With Ne^+, no $C_6H_5CN^{++}$ is found, so that the appearance potential of $C_6H_5CN^{++}$ must lie between 21.6 eV and 24.58 eV. For comparison, the appearance potentials of doubly ionized benzene, toluene and naphthalene all have the rather low values 26.0; 24.5 and 22.8 eV, respectively [46].

This appears to be the first known example of a charge exchange process $X^+ + A \rightarrow A^{++} + X + e$. Much less surprising is the occurrence of processes of the type $X^{++} + A \rightarrow A^{++} + X$, as reported, for example, in Ref. [34].

VIII. Conclusion

The present experiment constitutes a novel and direct way of measuring the dependence $k(E)$ of the unimolecular decomposition rate constant on the excitation energy. Conceivably, by employing primary mass selection and more sophisticated detection techniques like signal averaging, this method could be applied to a much larger variety of substances. This would open up the most direct experimental approach to unrevel the dissociation kinetics of complex systems.

Acknowledgments

We are indebted to the Deutsche Forschungsgemeinschaft for financial support in building the apparatus and to Prof. O. OSBERGHAUS for his interest and stimulating discussions.

[1] For a recent review, see H. M. ROSENSTOCK, Adv. Mass Spectrom. **4**, 523 [1968]; also: C. E. KLOTS, J. Phys. Chem. **75**, 1526 [1971].
[2] O. OSBERGHAUS and CH. OTTINGER, Phys. Lett. **16**, 121 [1965].
[3] CH. OTTINGER, Z. Naturforsch. **22 a**, 20 [1967].
[4] I. HERTEL and CH. OTTINGER, Z. Naturforsch. **22 a**, 40 [1967].
[5] I. HERTEL and CH. OTTINGER, Z. Naturforsch. **22 a**, 1141 [1967].
[6] A review has been given by E. LINDHOLM, in: Ion-Molecule Reactions in the Gas Phase, Adv. in Chemistry Ser. No. **58**, (Amer. Chem. Soc., Washington 1966), p. 1.
[7] A brief account of the present work has been given: B. ANDLAUER and CH. OTTINGER, J. Chem. Phys. **55**, 1471 [1971].
[8] For a review, see: B. S. RABINOVITCH and M. C. FLOWERS, in: Quarterly Reviews **18** (2), 122 [1964]. For NO_2, see also: H. GAEDTKE u. J. TROE, Z. Naturforsch. **25 a**, 789 [1970].
[9] In contrast, some very weak metastable peaks in acetylene double their intensity at a pressure of only $2 \cdot 10^{-7}$ Torr, see U. LÖHLE and CH. OTTINGER, Int. J. Mass Spectrom. and Ion Physics **5**, 265 [1970].
[10] W. B. MAIER II, J. Chem. Phys. **42**, 1790 [1965].

[11] R. F. STEBBINGS, B. R. TURNER, and J. A. RUTHERFORD, J. Geophys. Res. **71**, 771 [1966].

[12] Unfortunately, symmetric charge exchange processes, e. g. $Ar^+ + Ar \rightarrow Ar + Ar^+$, could not be used for this calibration, since the secondary ions would have been difficult to distinguish from those primary ions which originate in regions in the ion source with a potential close to the molecular beam potential (see Fig. 2).

[13] Table 4 contains a few examples of ions suspected to originate from Penning ionization. As a test, in that case all primary ions were blocked off by changing the ion source potentials appropriately. Although this did suppress the secondary ions in question, it is not a proof against Penning processes taking place, because changing the ion source conditions might also have reduced the yield of excited neutrals.

[14] See E. W. MCDANIEL, Collision Phenomena in Ionized Gases, J. Wiley, New York 1964, Table IV, p. 732 ff.; E. E. MUSCHLITZ, Science **159**, 599 [1968]; V. CERMÁK, J. Chem. Phys. **44**, 1318 [1965]. Other long-lived states with excitation energies close to the I. P. are also unlikely to contribute (H. HOTOP, private communication).

[15] This is, for example, very important for the reaction $Kr^+ + C_6H_5CN$, where a small impurity of air in the krypton would lead to a spuriously small satellite: main peak intensity ratio (see Figs. 4 and 5).

[16] E. STIEFEL, Einführung in die numerische Mathematik, B. G. Teubner, Stuttgart 1961, p. 52.

[17] Catalog of Mass Spectral Data, American Petroleum Institute, Research Project No. 44, Carnegie Institute of Technology, Pittsburgh (Pa.) 1953.

[18] M. B. WALLENSTEIN and M. KRAUSS, J. Chem. Phys. **34**, 929 [1961].

[19] W. A. CHUPKA, J. Chem. Phys. **30**, 191 [1959].

[20] J. L. FRANKLIN, J. G. DILLARD, H. M. ROSENSTOCK, J. T. HERRON, K. DRAXL, and F. H. FIELD, Ionization Potentials, Appearance Potentials, and Heats of Formation of Gaseous Positive Ions, NSRDS-NBS 26, U.S. Govt. Printing Office, Washington 1969.

[21] In Ref. [4], 15.2 eV is given as A.P. ($C_6H_4^+$); this refers to "normal" fragments $C_6H_4^+$; according to [4] the A.P. for $C_6H_4^+$ as a "metastable" is lower by 1.3 eV.

[22] The main peak could not be used for this experiment because it was largely due to charge exchange with Xe^{++}. Furthermore, the large excess of parent ion in the $Xe^+ + C_6H_5CN$ mass spectrum caused a contribution to the satellite peak on mass 76 from collision-induced dissociation, which had to be subtracted.

[23] Of course, for an endothermic process the ion yield must eventually tend to zero with decreasing impact energy. For the very small endothermicity in the present case this portion is below the accessible energy range.

[24] A measurement of SP/MP at a higher value of the drawout-field F would obviate these assumptions by providing additional experimental information, but is not feasible because of the broadening of both peaks with increasing F.

[25] In addition to these factors, the relative contributions from RE = 14.0 and 14.7 eV were multiplied by the abundance ratio $Kr^+(^2P_{3/2})/Kr^+(^2P_{1/2}) = 2:1$ (see Ref. [6] and Table 1).

[26] B. ANDLAUER, Diplomarbeit, Freiburg 1970.

[27] For charge exchange with CO^+, the mass 76 main peak intensity varied with U_{ion} almost exactly as for the Kr^+ charge exchange (the same is true for the satellite peak intensities, respectively). For CO^+ no reduction to obtain $Q(U_{ion})$ was attempted because of the complications by the comparatively minor contributions from RE 16.8 eV. It is very likely, however, that the relative cross section for mass 76^+ formation by CO^+ impact approximately follows curve (c) (RE = 14.0 eV).

[28] F. H. MIES and M. KRAUSS, J. Chem. Phys. **45**, 4455 [1966].

[29] D. L. BUNKER, J. Chem. Phys. **40**, 1946 [1964].

[30] See Eq. (1) in [4]; the additive term −21.7 merely results from the uncorrected U_{el} scale used in that paper.

[31] Similar, but much less direct evidence for incomplete energy randomization can be found in: U. LÖHLE and CH. OTTINGER, Int. J. Mass Spectrom. and Ion Physics **5**, 265 [1970].

[32] CH. OTTINGER, Z. Naturforsch. **20 a**, 1229 [1965].

[33] C. LIFSHITZ and B. G. REUBEN, J. Chem. Phys. **50**, 951 [1969].

[34] Similar considerations concerning the influence of the $k(E)$ cutoff position on the ratio metastable: normal fragment ions were already presented in Refs. [4] and [5].

[35] B.-Ö. JONSSON and E. LINDHOLM, Ark. Fysik **39**, 65 [1969].

[36] B. BREHM, Z. Naturforsch. **21 a**, 196 [1966].

[37] The possible objection that $C_4H_4^+$ might be formed by endothermic charge exchange with $Kr^+(^2P_{3/2})$, RE = 14.0 eV, was disproved by measuring the relative yields I(14.0) and I(14.7) at RE = 14.0 and 14.7 eV, respectively, as a function of the Kr^+ translational energy $e\,U_{ion}$. Between $U_{ion} = 20$ and 250 V the ratio I(14.0)/I(14.7) increased by only 5%.

[38] H. M. ROSENSTOCK and M. KRAUSS, Adv. Mass Spectrom. **2**, 251 [1963].

[39] E. GUSTAFSSON and E. LINDHOLM, Ark. Fysik **18**, 219 [1960].

[40] E. W. MCDANIEL, Collision Phenomena in Ionized Gases, J. Wiley, New York 1964.

[41] R. S. LEHRLE, J. C. ROBB, J. SCARBOROUGH, and D. W. THOMAS, Adv. Mass Spectrom. **4**, 687 [1968].

[42] V. L. TALROSE, Pure and Appl. Chem. **5**, 455 [1962].

[43] E. F. GURNEE and J. L. MAGEE, J. Chem. Phys. **26**, 1237 [1957].

[44] P. C. HAARHOFF, Mol. Phys. **7**, 101 [1963].

[45] G. Z. WHITTEN and B. S. RABINOVITCH, J. Chem. Phys. **38**, 2466 [1963].

[46] M. VESTAL, A. L. WAHRHAFTIG, and W. H. JOHNSTON, J. Chem. Phys. **37**, 1276 [1962].

[47] F. H. DORMAN u. J. D. MORRISON, Canad. J. Phys. **35**, 575 [1961].